ACCEPTED VERSION of the peer-reviewed article
Authors acknowledge the original source of publication:

Separation of H_2 and CO_2 Containing Mixtures with Mixed Matrix Membranes Based on Layered Materials
Rubio, Cesar; Zornoza, Beatriz; Gorgojo, Patricia; Tellez, Carlos; Coronas, Joaquin
Current Organic Chemistry
VOLUME: 18
ISSUE: 18
Page: 2351 - 2363
2014
http://www.eurekaselect.com/node/123806/article

The published manuscript is available at EurekaSelect via
http://www.eurekaselect.com/openurl/content.php?genre=article&doi=10.2174/13852728196661408062011 32

Separation of H_2 and CO_2 containing mixtures with mixed matrix membranes based on layered materials

César Rubio,[a] Beatriz Zornoza,[a] Patricia Gorgojo,[b] Carlos Téllez,[a] Joaquín Coronas[a,*]

[a]Chemical and Environmental Engineering Department and Instituto de Nanociencia de Aragón (INA), Universidad de Zaragoza, 50018 Zaragoza, Spain

[b]The School of materials, The University of Manchester, Oxford Road, Manchester M13 9PL, UK

*Corresponding author: coronas@unizar.es

Abstract

Some membrane separation processes are gradually taking over conventional processes such as distillation, evaporation or crystallization as the technology progresses from bench-scale tests to large-scale prototypes. However, membranes for H_2 and CO_2 separation constitute a daring technology still under development. This overview focuses on mixed matrix membranes (MMMs), a special type of membranes in which a filler is dispersed in a polymer matrix, as a successful strategy to improve their permeability-selectivity performance while keeping the polymer processability. In particular, among all the possible fillers for MMMs, layered materials (porous zeolites and titanosilicates and graphite derivatives) are discussed in detail due to the several advantages they offer regarding selective microporosity, crystallinity and, what is most important, high specific surface area and aspect ratio. In fact, a selective and as thin as possible, i.e. with high aspect ratio, filler would help to develop high performance MMMs.

Keywords: Layered material, Zeolite, Titanosilicate, Graphite, Graphene, Graphene oxide, Mixed matrix membrane, Gas separation.

Introduction

The separation of H_2, related to hydrogen economy, and CO_2, because of environmental concerns, containing mixtures under practical conditions is still a challenge to be addressed.

In the large scale production of H_2 several other gases are generated along with it. The corresponding gas mixtures, mostly H_2/CO_2 (from the transformation of coal and oil heavy fractions) and H_2/CH_4 (from the steam reforming of CH_4) [1], are difficult to separate and the purification processes involved often require high energy inputs. Currently, the purification of H_2 is carried out by adsorption processes such as pressure swing adsorption [2] and cryogenic distillation [3]. However, this last process gives rise to low purity H_2 ($\leq$95%). Regarding CO_2 separation when oriented to climate remediation, large point sources like coal-based power plants, natural and synthesis gas processing plants and cement plants are identified as the key places for cost-effective capture [4]. With regard to combustion processes, three different approaches to capture CO_2 can be identified: pre-combustion [5], post-combustion [6] and oxyfuel combustion [7]. Amine-based processes constitute a commercial technology for CO_2 capture in post-combustion; however, the huge volumetric streams that need to be treated under this new paradigm of CO_2 remediation claim for alternatives. Besides, these processes are highly energy intensive because of the high regeneration energy consumption. In any event, the separation of CO_2/N_2 gas mixtures would represent the approach to post-combustion, whereas, pre-combustion generally relates to coal gasification where H_2/CO_2 mixtures (above mentioned) are generated. In oxyfuel processes the use of pure oxygen results in a flue gas containing only CO_2, and in this case the main energy penalty would come from the production of O_2 from air, something which could also be addressed by membrane technology [8].

Many opportunities for replacing some of the above mentioned processes (adsorption, cryogenic distillation, absorption) will certainly arise for membrane technology based on the following aspects [9-13]:

i) Better energy efficiency than other classical processes.

ii) Possibility of being costly competitive even at low scale.

iii) Simplicity of operation.

iv) Portability and operation compactness, what is in part related to process intensification and its advantages [14].

v) Easy to scale up by adding parallel units.

vi) Benign character for the environment.

From the mere commercial point of view, membrane technology for gas separation is dominated by polymeric materials [9]. Nevertheless, this type of membranes, even though they are more versatile and cheaper than those made of ceramics or metals, has a limitation concerning the maximum selectivity values which can be reached for some particular industrial processes (e.g. separation of air or the mixtures we are dealing with) [10, 15]. This is why a few years ago mixed matrix membranes (MMMs) were introduced as a new kind of composite membranes aiming at the improvement of the separation performance of pure polymer membranes. MMMs are polymeric membranes in which a filler (typically porous) is homogeneously dispersed to improve as much as possible the permeability-selectivity binomial for a given separation with minor alterations in the polymer processability. Many porous materials have been used as fillers, namely, activated carbons [16], zeolites [17], ordered mesoporous silicas [18], layered silicates [19], and MOFs [20], to go beyond the empirical upper bounds established for each gas pair of interest [10].

From an extensive literature review and our own experience, the filler for a MMM must have as many as possible of the following properties:

i) Ordered porosity, since it allows the formation of strong nanocomposites with a good matching between the pore size and the polymer chain diameter [21].

ii) Adequate chemical composition to enhance filler-polymer interaction; this is of particular interest when metal-organic fillers are used since their organic moieties would present better interaction with polymers [22].

iii) Textural properties; this means abundant concentration of surface groups (as silanols in ordered mesoporous silicas) for interaction with polymer functionalities [21, 23].

iv) Appropriate shape to minimize agglomeration, for instance, by using spheres (particles that are stacked with the lowest contact surface [21]) or to maximize filler-polymer contact area by using an exfoliated clay-type filler [24].

v) Nanosize to enhance filler-polymer interaction through external surface area and also in some cases to reduce the membrane thickness through the preparation of asymmetric thin nanocomposite MMMs [25].

vi) Selectivity, the filler in general must be micro or mesoporous and/or present specific interaction with the fastest permeating molecule in the mixture since the final goal is to improve the membrane performance.

All these six properties might not be available in the same filler; this is the reason behind a very recent new strategy in which two fillers of different chemical nature and shape are dispersed in the same continuous polymer matrix with the aim of producing synergy effects [26, 27].

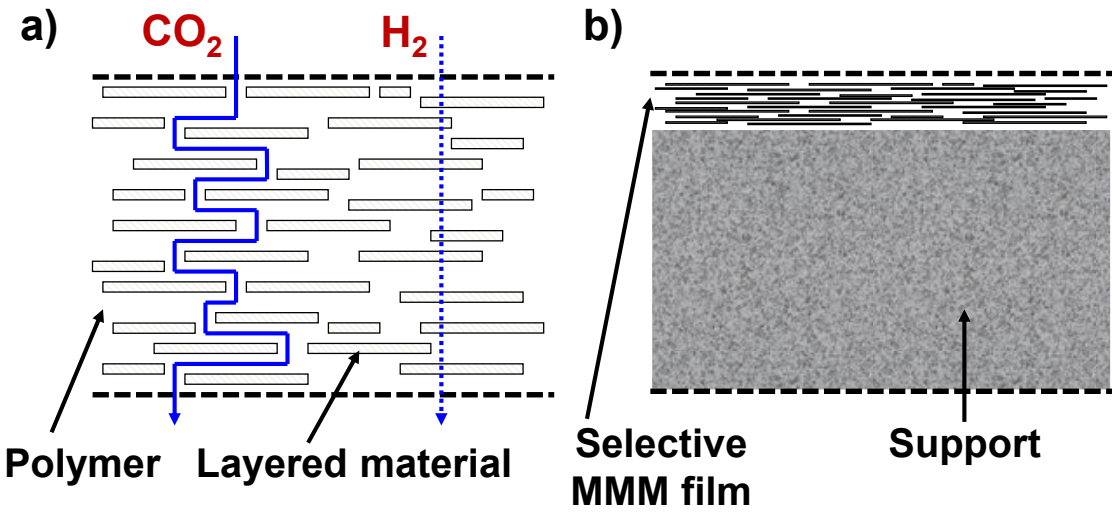

Figure 1. a) Scheme of dense MMM containing a layered material filler selective for H_2 permeation; b) scheme of an asymmetric membrane with a selective MMM thin film deposited onto a porous support. The separation mechanisms in both types of membranes relate to either differences in kinetic diameters of permeating molecules (the kinetic diameters of common permanent gases such as He, H_2, CO_2, O_2, N_2 and CH_4 are 2.6, 2.9 and 3.3, 3.46, 3.64 and 3.8 Å, respectively) or to preferential adsorption of one of the components in the mixture (as in CO_2 containing mixtures).

In any event, from the plethora of fillers that can be used in MMMs, layered materials (lamellar zeolites and titanosilicates and graphite and its derivatives) can benefit from most of the previous desirable features and are discussed in detail in this review. MMMs can be considered a special kind of nanocomposites [28] where the interaction between the filler and polymer gives raise to better separation properties. Layered zeolites and titanosilicates are microporous (e.g. materials with pore diameters less than 2 nm) crystalline materials that can be delaminated to decrease their size and

thickness and thus increase their aspect ratio, something that usually is accompanied by an important increase of specific surface area. These characteristics are of paramount importance when the goal is the production of more efficient supported MMMs in which a very thin selective layer is formed on top of a porous substrate [29, 30] as to increase permeance and preserve the selectivity values of their analogous dense MMMs (Figure 1). Regarding graphene (or the more practical few-layered graphene, i.e. FLG), although it is impervious to all molecules in its defect-free form, defects produced during the preparation of FLG [31] could be useful to obtain selective membranes as will be discussed below.

To conclude, some of these layered materials, as titanosilicates [32] and graphite derivatives [33] can be synthesized and modified without the use of expensive organic molecules or just by simply mechanical processing, what makes their use ecofriendly.

Layered silicates, zeolites and pseudozeolites

Traditional molecular sieving materials frequently have an aspect ratio (particle length/particle thickness) of ca. 1. The geometry of these fillers is not practically affected by the orientation within the polymer phase but limits the formation of thin selective layers [34]. Recent developments have used high aspect ratio (> 10) sieving materials (usually known as layered materials, fakes or platelets) as alternative fillers to traditional sieves in hybrid membranes [24, 35-37]. The features of layered materials such as high aspect ratio and small thickness can improve the separation performance by adding only a small volume fraction of these fillers within the MMM. In this case, the permeation of large molecules is hindered due to the more tortuous pathways that they have to follow, i.e. they cannot easily pass through the pores, whereas small molecules permeate very fast due to the small thickness [24] as depicted in Figure 1. Another field of application of these materials is drug delivery [38, 39]. For instance, with Poly(d,l-lactide-co-glycolide)/montmorillonite nanoparticles it has been developed a novel bioadhesive drug delivery system for oral delivery of anticancer drugs [40].

Exfoliation or delamination is a challenging process associated with layered materials. Layers are held together by charge neutralizing anions or cations or by the structuring agents employed during their synthesis. This process consists of a first step of swelling by intercalation of an organic surfactant, such as quaternary alkyl ammonium ions or amine molecules by ion exchange or hydrogen-bonding interaction with intergallery moieties. This is followed by an appropriate exfoliation technique such

as sonication and a final activation step by chemical extraction or calcination. Upon pillaring or exfoliation/delamination the accessibility of the platelets increases (the external surface area can be about 10 times higher than that of the parent zeolite) [41] and their thermal stability, homogeneous distribution of pores and acidic character are preserved [42]. Layered materials can therefore be exfoliated into individual sheets of few-layered nanostructures providing many functional sites which have enormous interest as catalysts [43, 44]. They have also been proposed for enzyme immobilization on their very high, hydroxylated and ordered external surface [45], adsorption of carbon dioxide by functionalization [46], and enhancing the selective properties of polymer membranes [35].

To take advantage of the favorable characteristics of these materials when embedded within a polymer in a MMM, these stacks of layers must be disrupted to yield an exfoliated state [34], and to use the geometric benefits of nanoplatelet molecular sieve. It is also critical that the face of the particles is oriented orthogonal to the direction of molecular transport [47, 48]. In addition, the exfoliated platelets reduce the fractional free volume (FFV) of polymer and the interfacial interactions between both phases; hence affecting the sorption of more condensable penetrants in the MMMs while reducing the available sorption sites for gas molecules [29].

Numerous molecular sieving platelets of different nature have been identified as potential filler materials in membrane applications [24, 47], and in particular in the preparation of MMMs: layered zeolites (MCM-22P [49], PREFER [50] and Nu-6(1) [51], and their corresponding delaminated zeolites ITQ-2 [43], ITQ-6 [52] and ITQ-18 [53], respectively, or MFI nanosheets [54]); layered silicates (Na and Sr silicate AHM-3 [55]) including the impermeable nanoclays [47, 56]; pseudozeolites (layered aluminophosfate, AlPO) [24]; and titanosilicates (JDF-L1) [57]. In Table 1 MMMs prepared with different flakes (layered silicates, zeolites and pseudozeolites) are classified and a detailed discussion will be presented below.

The concept of selective flakes emerged as an extension of the concept of impermeable layers or nanoclays, silicate materials which have intensively been used to reinforce the polymer matrix due to their low cost, easy accessibility and environmentally friendliness [58]. Cussler's group investigated barrier membranes with differently aligned flakes confirming that thin mineral platelets with a certain size distribution diminished gas permeability [6, 47].

Table 1. Gas separation MMMs comprising layered silicates, layered zeolites and layered pseudozeolites.

Layered material (layered precursor)	**Delaminated/ exfoliated flake**	**Example of MMM (flake/polymer)**	**Applied separation**
Clays		Sepiolite/PDMS [59] Montmorillonite/PEI [60] Hectorite/PEI [34]	CO_2/CH_4 CO_2/CH_4 -
Na/Sr-AMH-3 silicate		Swollen AMH-3/PBI [61] Swollen AMH-3/CA [62]	H_2/CO_2 CO_2/CH_4
Zeolite MCM-22P (precursor of MCM-22)	ITQ-2 [43]	MCM-22/PBI [61]	H_2/CO_2
Zeolite PREFER (precursor of ferrierite)	ITQ-6 [52]	-	-
Zeolite Nu-6(1) (precursor of Nu-6(2))	ITQ-18 [53] Exfoliated Nu-6(2) [42]	Nu-6(2)/PSF [63] Nu-6(2)/PI [64] Exfoliated Nu-6(2)/co-6FDA [65]	H_2/CH_4 H_2/CH_4 H_2/CH_4 O_2/N_2
MFI nanosheet (multillamelar silicalite-1)		Hybrid bulk MFI-layered MFI/PI [54]	CO_2/CH_4
AlPO		AlPO/co-6FDA [24] Swollen AlPO/PE [66]	CO_2/CH_4 O_2/N_2 H_2/CO H_2/CO_2

A single sheet of a typical clay mineral material has a thickness of one to few nanometers and hundreds to thousands nanometers in extent and its structure typically comprises crystalline octahedral aluminum and tetrahedral silicon sheets. They can be categorized into five main types, namely smectite, illite, kaolinite, chlorite or sepiolite. Several techniques that have been used to produce traditional clay-polymer MMMs can be extended to layered zeolites; before homogeneously dispersing the clay in the polymer, surface modification of clays by the intercalation of an organic compound is commonly done to enhance particle dispersion and exfoliation into individual sheets [67]. This approach is usually combined with more environmentally friendly processes:

melt-blending or in situ polymerization, in order to incorporate the filler into the polymer matrix [68]. This process involves annealing above the softening point of the polymer to allow the penetration of polymer chains into the galleries of the silicate layers. Defontaine et al. [59] prepared sepiolite/PDMS MMMs, with PDMS chains covalently linked through the formation of Si-O-Si bonds between the filler particles and the polymer chains due to the silanol groups in the clay structure. By using this layered silicate with approx. 3.7-10.6 Å cavity size an increase in CO_2/CH_4 selectivity up to 145% (sacrificing the permeability) was achieved compared to the pure PDMS membrane. Hashemifard et al. [60] incorporated organically modified montmorillonite into PEI to prepare asymmetric MMMs through the dry/wet phase inversion method showing 28% increment in CO_2/CH_4 selectivity as compared to the pure PEI. In addition, synthetic hectorite of 1 nm thick and 25-30 nm long was dispersed in PEI with the aim of fabricating asymmetric hollow fibers [34].

The porous layered silicate AMH-3 ($Na_8Sr_8Si_{32}O_{76}\cdot 16H_2O$), synthesized without the use of organic structure-directing agent (OSDA), is an attractive candidate to fabricate selective MMMs. It has 8-membered ring (MR) (i.e. eight [SiO_4] tetrahedra ring) pores in all three principal crystallographic directions with nominal pore opening of 3.4 Å [55]. Conventional methods for clay swelling were not effective with AMH-3, swelling constituting the main obstacle to enhance the interlayer spacing needed for MMMs [62]. Choi et al. [35] synthesized proton-exchanged AMH-3, prepared under mild conditions by ion exchange of Sr and Na cations in the original AMH-3. An aqueous solution of histidine was used for this purpose, and subsequent sequential intercalation of dodecylamine led to swollen AMH-3. They introduced this silicate material in a continuous phase of PBI selective matrix by means of a priming protocol after which the sheet-like AMH-3 showed a random orientation. The swollen AMH-3 MMMs presented a significant reduction in CO_2 permeability with only 3 wt% of loading. In contrast, substantial enhancement of H_2/CO_2 selectivity was found compared to pure PBI membranes (from 15 to 40) measured at 35 ºC, possibly due to the improvement of the polymer properties at silicate-polymer interfaces or to the molecular sieving role of the silicate. However, when testing these membranes at 100 and 200 ºC similar selectivities to those of pure polymer were obtained.

In a recent study, Kim et al. [62] delaminated swollen AMH-3 into flakes by a high-shear mixer during blending in solution with cellulose acetate (CA). This technique guaranteed a high degree of exfoliation of AMH-3 layers in the polymer

phase unlike conventional dispersion methods like sonication and stirring. By shear stress mixing they obtained a higher degree of exfoliation, and stacks of only 4-8 AMH-3 layers were measured by TEM and SAXS. In this case gas separation measurements showed a high increase of CO_2 permeability while maintaining the CO_2/CH_4 selectivity even at low loadings (2-6 wt%) of swollen AMH-3. This result was attributed to the effect of AMH-3 pores as well as interlayer mesopores present in the exfoliated AMH-3 layers.

MCM-22P is the layered precursor of the framework zeolite MCM-22 (with the MWW type structure). The latter comprises 10 MR channels in the plane of the layers (*a*- and *b*- axes) and small 6 MR openings perpendicular to the layers (along the *c*-axis) [49]. In 1998 Corma et al. [43] reported the modification of MCM-22P by surfactant intercalation and exfoliation of the resulting material to single layers. The new delaminated material ITQ-2 with high external surface area (> 700 m^2/g) was obtained. By pillaring MCM-22 after a swelling process the material MCM-36 was produced [69]. ITQ-2 results an attractive material for high performance heterogeneous catalysis, because of its large surface density of active sites. Also, it is useful as a molecular sieve for H_2, due to its *c*-out-of-plane orientation of the layers with 6 MR pores. Membranes of MCM-22 crystals were prepared by several cycles of layer-by-layer (LBL) depositions on α -alumina substrates [70]. To fill the microscopic defects between the MCM-22 coated layers mesoporous silica was deposited by evaporation induced self-assembly (EISA). Due to the plate-like structure and significant interlayer interactions, the 6 MR pores were also found aligned perpendicular to the substrate providing a high H_2/N_2 separation selectivity of 120.

Regarding MMMs, MCM-22 plate-like crystals were embedded within a PBI matrix and applied for H_2/CO_2 separation [61]. A significant reduction in permeability was observed due to an increase of tortuosity of diffusion paths, which was a direct consequence of the high aspect ratio of the layered filler. In addition, no selectivity enhancements compared to that of pure polymer membranes were found.

Other exfoliated zeolites such as ITQ-6 and ITQ-18 have been obtained from layered zeolites PREFER and Nu-6(1), respectively [52, 53]. Analogously to MCM-22P, layered Nu-6(1) can be converted by calcination into the framework zeolite Nu-6(2). The synthesis of Nu-6(1) was first reported by Whittam in the early 1980s by using 4,4´-bipyridine as the SDA [71]. Nu-6(1) can be described by a model in which layers are formed by $[SiO_4]$ and $[SiO_3OH]$ tetrahedra and where two

crystallographically independent 4,4′-bipyridine molecules are localized in the interlayer or gallery space [51], as shown in Figure 2. On the contrary, the hexamethylenimine molecules used for the crystallization of zeolite MCM-22P are found both in between the layers and inside the galleries [72]. By removing the 4,4′-bipyridine template, Nu-6(1) is transformed into Nu-6(2) [53]. Zeolite Nu-6(2), with NSI type structure, has been used as a catalytic material for dewaxing, disproportionation and isomerization [51], and due to its small 8 MR pores (3.2 x 4.3 Å and 2.4 x 4.8 Å, depicted also in Figure 2 as A and B) and plate-like growth habit has been applied to the preparation of zeolite-polymer MMMs for selective H_2 permeation [63].

Delaminated Nu-6(1) has BET specific surface areas of ca. 500-600 m^2/g, while that of framework zeolite Nu-6(2) is about 80 m^2/g [53]. Gorgojo et al. prepared Nu-6(2) powder with Si/Al ratio of 45 and 52.5 m^2/g [63] which was directly exfoliated, that is, without previous intercalation or swelling stage. The exfoliation took place in the presence of Na^+ and CTA^+ (cetyltrimethylammonium) ions at mild pH (~9) and room temperature and gave rise to a porous material with a BET specific surface area of around 300 m^2/g [42]. Figure 3a shows a SEM image of Nu-6(2) particles with an inset of a TEM image of the aforementioned exfoliated Nu-6(2), a thickness of ca. 5 nm is observed.

Nu-6(2) was embedded in two different polymers (PSF and PI) [64] whereas exfoliated Nu-6(2) was added to copolyimide 6FDA-4MPD/6FDA-DABA (co-6FDA) [65]. Nu-6(2) based MMMs were free of interfacial voids between both phases due to the high Si/Al ratio of the zeolitic filler (45 what in turn means hydrophobic character) Superior separation performance of these MMMs was achieved in comparison with the bare polymers. This improvement was attributed to the molecular sieve role played by the high aspect ratio of Nu-6(2) which has, as already mentioned, two types of 8 MR channels with limiting dimensions of 2.4 and 3.2 Å (Figure 2). Increases in permeability (P_{H2} = 49.4 Barrer) and H_2/CH_4 selectivity (206) for 15 wt% Nu-6(2)-PI MMMs were obtained compared to the pure polymer (P_{H2} = 31.9 Barrer; H_2/CH_4 selectivity = 118) [64].

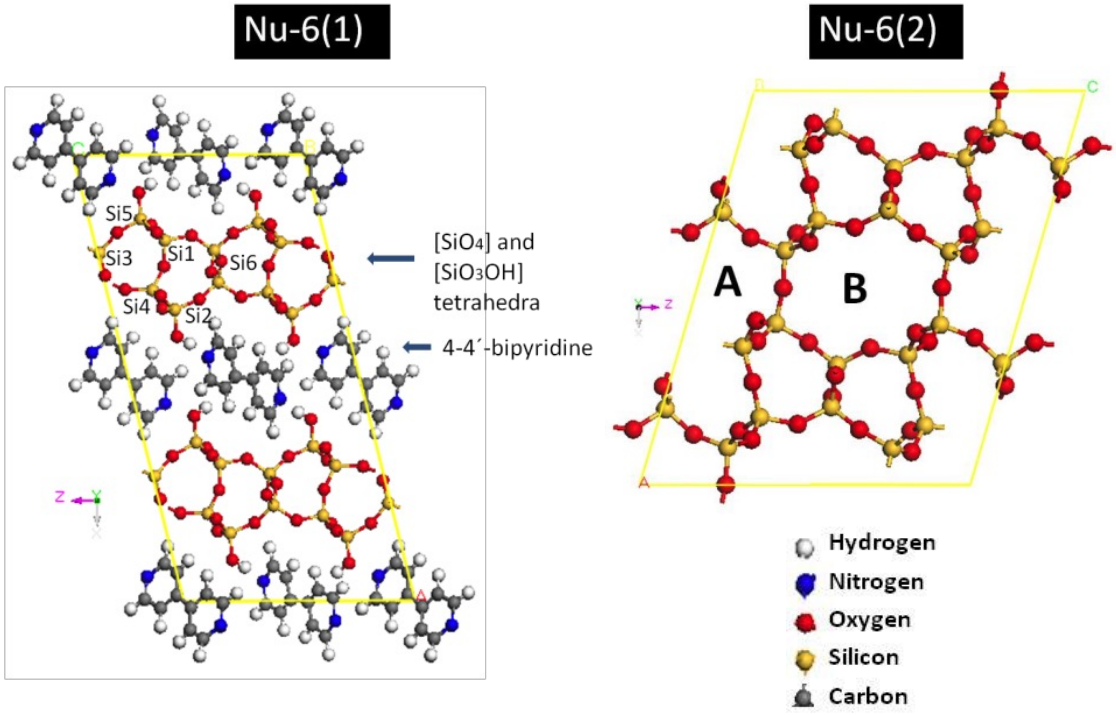

Figure 2. Representation of the structures of Nu-6(1) and Nu-6(2). Layered Nu-6(1) is formed by [SiO_4] and [SiO_3OH] tetrahedra with two crystallographically independent 4,4´-bipyridine molecules that are localized in the interlayer space. The framework structure of Nu-6(2) has straight 8 MR channels running along the [010] direction. Two non-equivalent sets of 8 MR channels alternating along the crystallographic *c*-direction are referred as A and B, having aperture distances of 3.2 x 4.3 Å and 2.4 x 4.8 Å, respectively. Thus, Nu-6(2) may be selective to H_2 molecules (kinetic diameter, 2.9 Å) limiting the passage of larger molecules. Materials Studio 4.3 from Accelrys® used to represent the structures by using data reported previously by Zanardi et al. [51].

Concerning exfoliated Nu-6(2) MMMs the interaction of the polymer and the filler was investigated by employing copolyimides with different carboxyl group concentrations. In particular hydrogen bonding was found to take place between the hydroxyl groups on the surface of the zeolite and the carboxylic groups of the polymer. In this case, separation tests were performed for H_2/CH_4 and O_2/N_2 mixtures. Figure 3b shows the H_2/CH_4 separation performance of MMMs composed of loadings up to 10 wt% of exfoliated Nu-6(2) in the co-6FDA (4MPD:DABA molar ratio 4:1). A maximum value of H_2/CH_4 selectivity of 37.9 (with 500 Barrer of H_2 permeability) was achieved with a 5.3 wt% of exfoliated zeolite [65]. These results indicate that these

zeolite sheets, with a pore size between the kinetic diameters of the two molecules, are suitable for the separation of H_2 from CH_4.

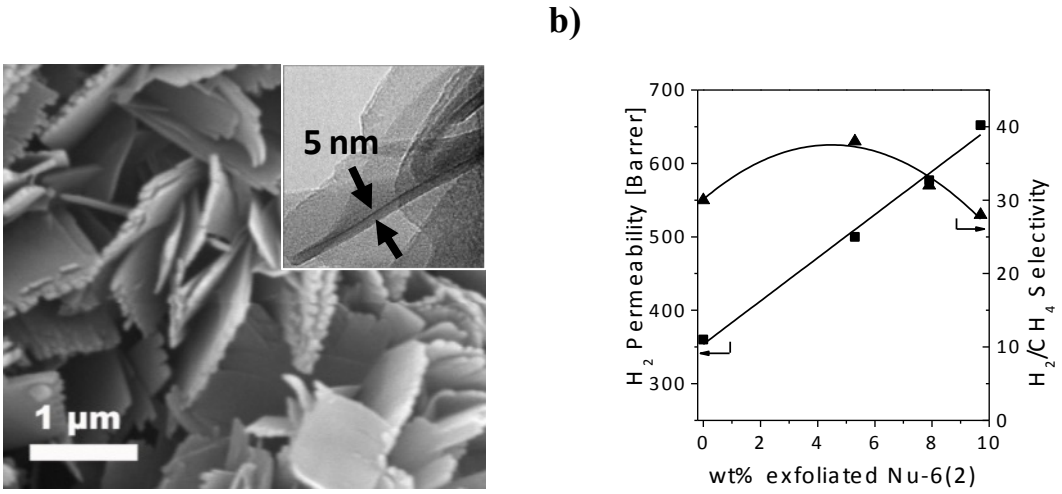

Figure 3. a) SEM image of Nu-6(2) crystals with high aspect ratio (0.06 x 1 x 1 µm). In the inset a TEM image of a thin particle of exfoliated Nu-6(2) is presented; b) H_2/CH_4 separation performance for MMMs comprising different exfoliated Nu-6(2) loadings and 6FDA-4MPD/6FDA-DABA (4MPD:DABA molar ratio 4:1) copolyimide. Lines are visual guides.

Another layered material that has been used for the fabrication of gas separation MMMs is layered silicalite-1 (MFI type zeolite structure). This material was obtained by using a new SDA, a diquaternary ammonium cation ($C_{22}H_{45}$-$N^+(CH_3)_2$-C_6H_{12}-$N^+(CH_3)_2$-C_6H_{13}) [54]. Thin (2 nm) silicalite-1 sheets were synthesized in a one-step hydrothermal reaction with the same pore size and local structure as conventional MFI type zeolite, i.e. 10 MR pores with a nominal pore size of 0.55 nm. This relatively larger pore size, in comparison to the previous AMH-3, MCM-22 and Nu-6(2), can be applied to the separation of bulkier molecules. For instance, exfoliated layered MFI/PS has been applied to xylene separations reaching a high *p*-/*o*-xylene separation factor of 65 [73]. Besides, layered MFI has also been combined with conventional MFI in the form of a hybrid material named BMLM (bulk MFI-layered MFI). This material has been added to PI polymer and has shown superior particle-polymer adhesion properties over the conventional MFI particles [54]. Moreover, BMLM MMMs performed better than membranes composed of conventional MFI particles and same polymers for CO_2/CH_4 separation.

Porous sheet-like structures are not only typical morphologies of some zeolites or silicates, but there are also other crystalline materials, such as pseudozeolitic materials which contain tetrahedrally coordinated phosphorous (aluminophosphates, AlPOs) [44, 74, 75]. In this case, AlPO sheets have a porous structure with rings of interconnected AlO_4 and PO_4 tetrahedra. In fact, the first selective flake-polymer nanocomposite membranes were fabricated by Jeong et al. [24] by embedding 10 wt% of intercalated layered AlPO within a hexafluorinated polyimide. These membranes showed substantially improved CO_2/CH_4 selectivity of 40.9 compared to 13.4 of the pure polymer. This enhancement in membrane performance was ascribed to the molecular sieving property of AlPO layers which favored the permeation of gases with smaller molecular dimensions. On the contrary, Vaughan et al. [36] did not achieve this molecular sieve effect with this same layered AlPO and other polymers such as PI, PSF, PDMS and CA. The authors pointed out the low dispersion of the platelets in the polymer and the inadequate exfoliation as the reason for poor improvement in membrane selectivity. Covarrubias et al. [66] swelled AlPO with CTA^+ and protonated octadecylamine (ODA). ODA-AlPO particles, added into PE matrix by in situ polymerization with metallocene catalyst were completely exfoliated. On the other hand, CTA-AlPO particles introduced into the polymer matrix via melt compounding had particles mainly in intercalated form with good preservation of the AlPO structure. CTA-AlPO/PE membranes with 5 wt% loading showed better H_2/CO separation performance, their H_2 selectivity values were in the range of 9.5-17.0 whereas those of pure PE were as high as 2.6. This better performance was due to the preservation of the porous structure of CTA-AlPO particles and good dispersion created through the melt mixing method, which makes these membranes promising for hydrogen purification applications.

Layered titanosilicates

Mixed octahedral-pentahedral-tetrahedral (OPT) microporous siliceous frameworks have been thoroughly studied since the early 1990s [76] and their synthesis has been inspired and motivated by many examples of such solids provided by Nature. These materials have a crystal structure consisting of tetrahedral units TO_4 (T= Si, Ge) and polyhedra MO_n (n= 5, 6) (M= Sn, Ti, Zr, V, Nb). ETS-10 [77] and ETS-4 [78] are probably the most studied members of this OPT family with, applications in catalysis, ion exchange, and separation processes [76]. However, there are only three layered OPT

titanosilicates: AM-4 [79], JDF-L1 [80] and jonesite [81], the last having scarcely been investigated.

JDF-L1 ($Na_4Ti_2Si_8O_{22}·4H_2O$) is a layered microporous titanosilicate with pore size of about 3 Å also reported as AM-1 [79, 82] and NTS titanosilicate [83]. Its structure was first obtained by Roberts et al. [80] in 1996 and more recently refined by Ferdov et al. [84]. The layers of JDF-L1 have 5 MR channels, running parallel to them ([100] or [010] equivalent directions, Figure 4a) which consist of four SiO_4 tetrahedra and one TiO_5 pentahedral pyramid, and 6 MRs composed of two square pyramids and two pairs of tetrahedra running along the [001] direction (Figure 4b) [80, 82]. Interestingly, small JDF-L1 crystals (3 × 3 μm) more suitable as filler for MMMs can be obtained by seeded hydrothermal synthesis [32] (Figure 4c).

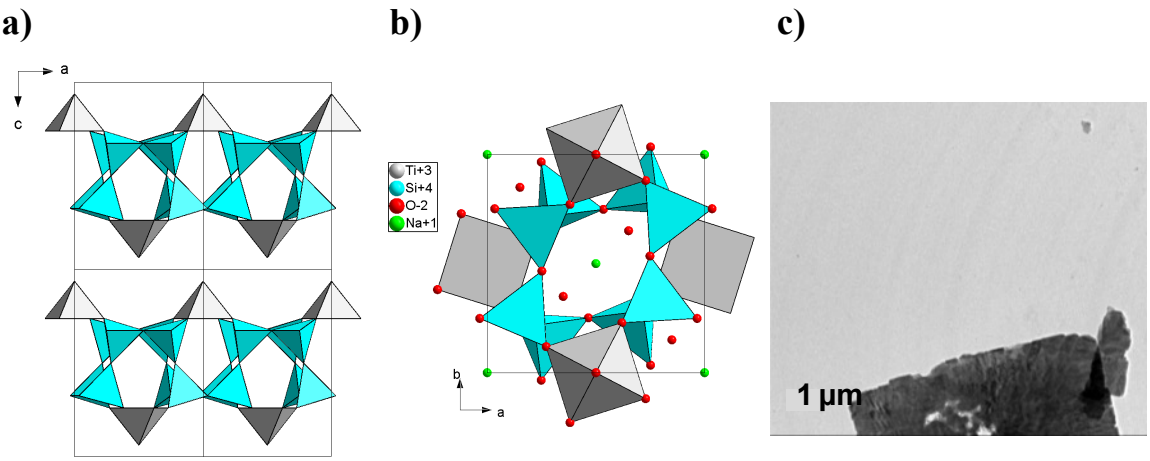

Figure 4. a) Structure of JDF-L1 along [010] direction where Na^+ cations and water molecules in the galleries have been removed to appreciate better the layered character of the material; (b) view along [001] direction where the 6 MR can be observed. Grey, TiO_5 square pyramids; blue, SiO_4 tetrahedra; red, oxygen atoms; green, Na^+ ions. Structures made with Diamond 3.2 using data reported previously by Roberts et al. [80]. c) TEM image of a sheet crystal of JDF-L1 obtained by seeded hydrothermal synthesis.

Galve et al. [85] used JDF-L1 to produce MMMs for H_2/CH_4 separation. They disaggregated JDF-L1 by means of CTA surfactant and combined it with co-6FDA (6FDA-4MPD/6FDA-DABA with 4MPD:DABA molar ratio 4:1). The disaggregation claimed by the authors (without swelling) made possible to obtain single, non-agglomerated sheet particles of JDF-L1, about 100 nm in thickness, keeping all the crystalline features of the as-made material and better dispersion properties for the

production of MMMs. In addition, a preferential horizontal orientation of the JDF-L1 particles dispersed into the polymer was observed (Figure 5), so that comparable improvements on the separation characteristics to those with higher loads of non-oriented particles could be achieved with smaller amounts of oriented particles. Galve et al. observed that during membrane casting high concentration polymer solution (13 wt%) led to a lower particle orientation, while a less viscous solution (10 wt%) allowed the filler to find a preferential horizontal orientation in the obtained MMM. This finding was corroborated by Raman spectroscopy, SEM and XRD, where MMMs showed peaks of JDF-L1 only related to the [*00l*] directions. Regarding the separation performance of these MMMs, CH_4 permeability decreased as a function of the JDF-L1 loading more drastically than that of H_2 which resulted in a remarkable increase of H_2/CH_4 selectivity. This effect was more pronounced for the membranes cast from a 10 wt% polymer solution, so that the maximum increase in H_2/CH_4 selectivity was achieved with a MMM containing 10 wt% of disaggregated JDF-L1. In this case the selectivity increased from 21.3 for the pure polymer to 35.6 in the MMM, the H_2 permeability values were 368 and 137 Barrer, respectively.

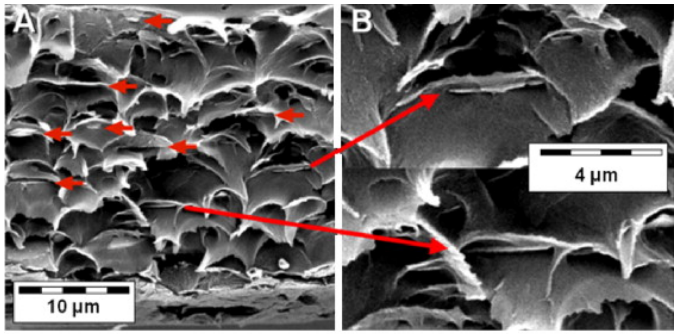

Figure 5. a) SEM images of the cross-section of a MMM containing 8 wt% JDF-L1 sheets. It can be observed the homogeneous dispersion of the sheets throughout the thickness as well as their orientation parallel to each other and perpendicular to the gas flow for optimum values of permeability and selectivity; b) magnification of two dispersed and horizontally oriented sheets. Reprinted from Journal of Membrane Science, 370, A. Galve, D. Sieffert, E. Vispe, C. Tellez, J. Coronas, C. Staudt, Copolyimide mixed matrix membranes with oriented microporous titanosilicate JDF-L1 sheet particles, 131-140, Copyright (2011), with permission from Elsevier.

Disaggregated JDF-L1 was also used to improve the dispersion of ca. 0.5 μm ordered mesoporous silica MCM-41 spheres in MMMs [26]. This study demonstrated that MMM performance could be enhanced by combining highly selective inorganic sheets with highly permeable inorganic MCM-41 particles with pores of 2-3 nm. In this case the layered titanosilicate JDF-L1 improved not only MMM selectivity but also the dispersion of the other filler. Membranes with a total amount of filler of 12 wt% and different calcined MCM-41 particles/JDF-L1 sheets weight ratios were tested for H_2/CH_4 separation. It was found that a small amount of JDF-L1 (2-4 wt%) made possible a more uniform distribution of the spheres throughout the cross-section of the MMM. With an 8/4 wt% MCM-41/JDF-L1 combined filler loading, H_2/CH_4 selectivity passed through a maximum (32.0), while maintaining a high level of H_2 permeability (440 Barrer). Pure polymer, 6FDA-4MPD/6FDA-DABA, showed a H_2/CH_4 selectivity of 18.9 and a H_2 permeability of 311 Barrer. The addition of MCM-41 particles to the polymer decreased selectivity and increased permeability, whereas the contrary was true for the addition of JDF-L1 sheets.

Like previously discussed layered zeolites and AlPOs, JDF-L1 can be swollen via intercalation reaction (with nonylamine) and a separation between the layers of 3 nm is achieved. After subsequent delamination via chemical extraction UZAR-S1 is obtained [57]. Even though JDF-L1 scarcely adsorbs N_2 (BET specific surface area is 30 m^2/g), UZAR-S1 presents a specific surface area of up to 204 m^2/g due to its fine particle size with high aspect ratio and thickness as low as 5 nm. UZAR-S1 was tested as a MMM filler with PSF [57], so that the nanometer-like particles produced upon the exfoliation step were observed by TEM into the membrane. Additionally, the presence of some aggregates indicated that, even though the swelling and exfoliation steps affect most of the precursor material, some particles with relatively large sizes would remain. Regarding the performance in terms of H_2/CH_4 separation of a MMM containing 4 wt% of UZAR-S1, H_2 permeability showed a small decrease from 11.8 to 11.5 Barrer, and H_2/CH_4 selectivity increased from 58.9 for pure PSF to 69.2 for the MMM. The improvement in the membrane separation ability relayed on the 6 MR pores that UZAR-S1 has along the [001] direction, so that the molecular sieving of its sheets was transferred to the composite membrane, favoring the transport of the smallest molecule.

The layered titanosilicate JDF-L1 was also used by Castarlenas et al. [86]. They processed swollen JDF-L1 with PSF by melt compounding to produce a master batch where JDF-L1 was partially exfoliated. This method, due to the partial absence of

organic solvents, is an environmentally friendly method for incorporating nanolayered silicates into polymer matrices and obtaining composite materials with enhanced mechanical and barrier properties [68]. The membranes with 2.3−9.5 wt% loading of inorganic layered material were characterized by TEM which corroborated the presence of very fine particles that had clearly been exfoliated. In addition, it was observed by XRD that the remaining, non-exfoliated JDF-L1 exhibited intensities corresponding to *00l* peaks, in agreement with the horizontal preferential orientation already observed by Galve at al. [85]. The good filler-polymer interaction was also evidenced by the shift of the characteristic band of PSF from 2·theta = 17.9° to 18.9°. This shift was attributed to the strong interaction between the matrix and the filler which gave rise to a reduction of the distance between polymer chains [27, 87]. As a consequence of the melt compounding, the crystallographic order of swollen JDF-L1 with a main peak at d-spacing = 3.0 nm was transformed into a broad, low intense peak centered at about d-spacing = 4.0 nm. This not only indicated JDF-L1 exfoliation but also the polymer chain penetration into the filler structure to form a composite. These d-spacing changes were also corroborated via TEM imaging. Besides, the melt compounding exfoliation process led to an increase in the average aspect ratio from 10.9 to 15.4. Regarding H_2/CH_4 separation, at filler loadings higher than 5 wt%, there was a continuous enhancement in H_2/CH_4 selectivity as the amount of inorganic filler increased, while a barrier effect clearly appeared. This finding supported the preservation of the porous layered structure of JDF-L1 upon the melt compounding process. In fact, H_2/CH_4 selectivity was increased from 58.9 (H_2 permeability = 11.8 Barrer) in pure PSF up to 128 (H_2 permeability = 12.5 Barrer) for the 8.3 wt% MMM; with higher loadings the selectivity decreased.

Since layered titanosilicates have scarcely been studied, we will comment on recent applications linked to JDF-L1 and AM-4. Pérez-Carvajal et al. [88] developed nanoarchitectures based on nanosheets of titanosilicate JDF-L1 doped with palladium and supported on glass fibers (GF). They applied the so called JDF-L1/GF material for H_2 adsorption up to 4 MPa and achieved a value of 0.9 wt%. As potential catalytic support, a mesoporous silica-pillared H^+-titanosilicate (SPT) was synthesized by Park et al. [89] in DDA-TEOS solution after calcination. In 2014 Park et al. [90] examined Ni/SPT and Rh/SPT loaded with 5 wt% metal as catalysts for partial oxidation of methane (POM) at 700 ºC obtaining H_2 yields higher than 90%.

AM-4 is a layered titanosilicate with similar potentialities than JDF-L1. It was first reported in 1997 [79] and its structure was established by Dadachov et al. [91] It is a monoclinic layered solid, with the molecular formula $Na_3(Na,H)Ti_2O_2(Si_2O_6)_2 \cdot 2H_2O$, built from TiO_6 octahedra and SiO_4 tetrahedra. It also contains intra- (in small cages within the layers) and interlayer Na^+ cations, and water molecules. In 2011 Casado et al. [92] developed an improved synthesis method of AM-4 crystals which enabled control of particle size by secondary growth and reduced synthesis time from 96 h to 6 h. A seeding step contributed to an additional decrease in the dimensions of the plate-like crystals from 0.55±0.13 x 6.9±0.8 to 0.05±0.02 x 1.2±0.2 μm without varying the morphology of the layers. Following a similar procedure to UZAR-S1, the delamination of AM-4 with nonylamine molecules gave rise to delaminated UZAR-S2 with BET specific surface area of 122 m^2/g and a CO_2 adsorption capacity of 0.22 mmol CO_2/g. Even though this value is about five times higher than that of original AM-4 is still lower than the value obtained for the microporous titanosilicate ETS-10 (2 mmol CO_2/g) [93]. AM-4 has been applied as catalyst for the isomerization of glucose in water at 100 ºC, giving reaction rates and fructose yields higher than those observed for ETS-10 catalyst [94].

At the moment there are no published results of membranes made with AM-4 or UZAR-S2. However, a recent study, carried out with both JDF-L1 and AM-4, showed that these layered titanosilicates can be modified by ion exchange with Ag^+, Zn^{2+}, and Cu^{2+} to improve their biocide activity against Staphylococcus Aureus colonies [95]. The combination of sheet-like particles causing barrier effects in MMMs with the biocide activity could be used to develop new kinds of membranes and active packages.

Graphene and derivatives

Graphene is a two-dimensional material formed by sp^2 hybridized carbon atoms linked in a honeycomb lattice that has become the most studied nanomaterial since its discovery in 2003 [96]. Pristine monolayer graphene as well as other forms namely, few-layered graphene (FLG), graphene oxide (GO) and reduced graphene oxide (rGO) have been recently applied in a wide range of scientific fields due to their exceptional electrical, mechanical and optical properties.

Graphene is mainly used for the fabrication of electronic devices, conductive coatings (transparent electrodes in solar cells), flexible touchscreens, biomedical applications, and reinforced composite materials. Very recently some research groups

have started to explore the potential of graphene and graphene-derivatives as membrane materials [97]. It is a fact that pristine graphene, i.e. a defect free graphene flake, is impermeable to everything even He [98]. However, continuous films fabricated from few to hundreds of graphene and GO flakes stuck on top of each other show selective properties for various separations due to the space between graphene sheets and/or holes produced during the oxidation step. Nair et al. [99] showed that submicrometer-thick graphene oxide membranes have excellent barrier properties for gases and vapors but allow unimpeded permeation of water. This same research group recently published the application of graphene oxide membranes as molecular sieves with a sharp cutoff of 4.5 Å when in contact with water [100]. Han et al. [101] prepared an ultrathin (22-53 nm thick) graphene nanofiltration membrane by filtration of rGO on alumina discs for water purification and found high retention for organic dyes and moderate retention for ion salts. This range of membrane thicknesses is still far from the ideal situation where just one-atom-thick layer of graphene would be the selective layer itself as to minimize flow resistance and maximize flux (Figure 6). Some publications over the past few years have shown the potential application of pristine and chemically modified porous graphene for gas separation by using molecular dynamics (MD) simulations [102-109].

Some research groups have attempted the fabrication of pores on extremely thin graphene flakes, i.e. porous graphene, via the exposure to the focused electron beam of a TEM [110], and via ultraviolet-induced oxidative etching that can create pores slightly larger than 0.3 nm in micrometre-sized graphene membranes selective for H_2 and CO_2 over larger molecules like Ar, N_2, and CH_4 [111]. Both approaches are inaccurate and hard to control and only very small membrane areas can be produced, therefore their industrial-scale application would be limited. Very recently membranes of perforated double-layer graphene have been fabricated with nanopores in the range of 7.6 to 1000 nm drilled via focused ion beam (FIB) [112]. These membranes have been tested for H_2/CO_2 gas separation and those with the smallest pores (7.6 nm pore diameter and 4 % porosity) showed permeance values orders of magnitude superior to existing membranes, and selectivities (ca. 4.7) comparable to some conventional polymers or carbon molecular sieves.

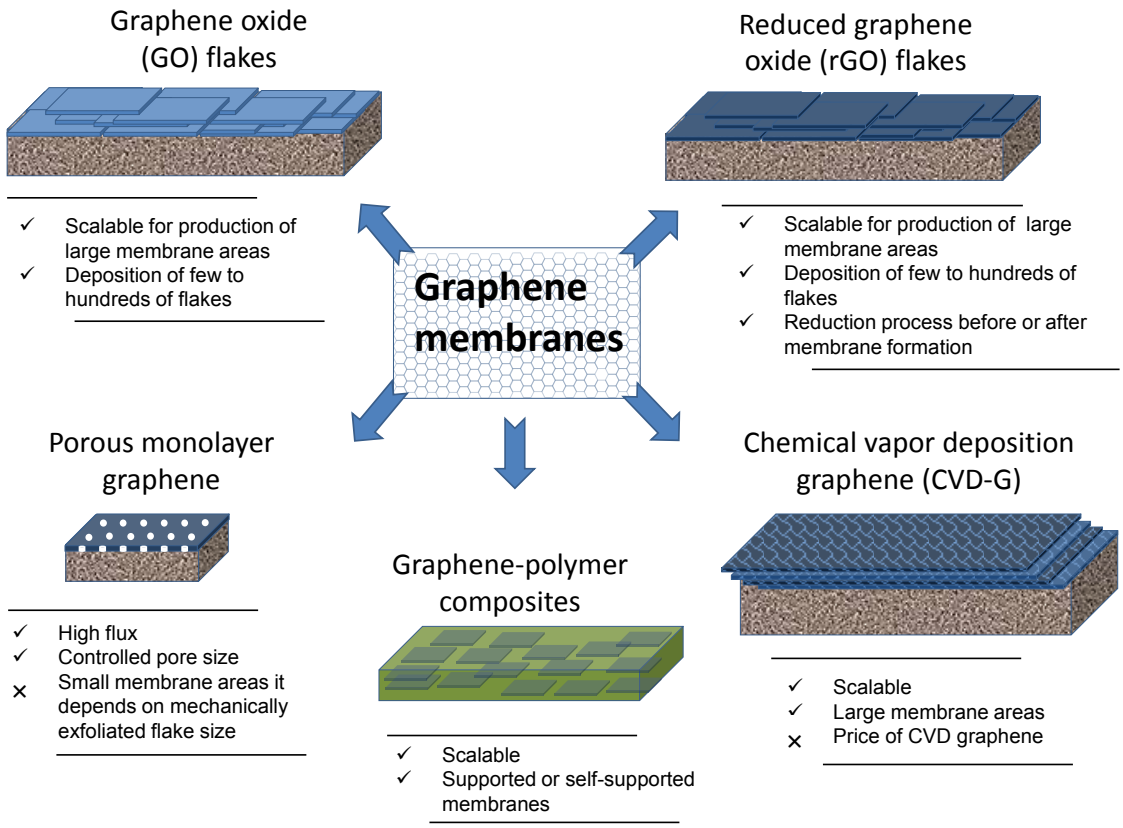

Figure 6. Schematic of different types of graphene-based membranes. Graphene oxide (GO), reduced graphene oxide (rGO), porous monolayer graphene and chemical vapor deposition graphene (CVD-G) are fabricated on porous substrates. GO and rGO flakes are deposited via filtration, CVD-G is transferred via a wet procedure using poly(methyl methacrylate) (PMMA), and porous graphene can be formed either by depositing mechanically exfoliated graphene using Scotch tape and etching or deposition of CVD-G and drilling with a focused ion beam (FIB). Polymer composites can be typically prepared by mixing the graphene in a polymer-solvent solution and casting or melt compounding.

More scalable approaches are two recently published works which have used very thin layers of graphene-based materials, such as graphene produced by chemical vapor deposition (CVD-G) and GO, on porous substrates [31, 113]. Promising performances for CO_2/N_2, H_2/CO_2 and H_2/N_2 mixtures with low transport resistance and high permeate flux were achieved and discussed below. Kim et al. showed that selective gas diffusion through FLG and GO membranes can be achieved by controlling gas flow channels and pores via different stacking methods [31]. One to five layers of CVD-G were transferred onto polymeric poly(1-methylsilyl-1-propyne) (PTMSP) supports, and

were tested for O_2/N_2. It was confirmed that CVD-G sheets are not impermeable to gases as they have defects such as tears and holes at grain boundaries. O_2/N_2 selectivity improved with increasing graphene stacking from 1.5 to 6, which suggests that gases diffused not only through defective pores on graphene but also between the interlayers. This phenomenon has been analyzed via the development of a gas transport model in a separate publication in which it has also been shown that the pore size of the porous support and its permeance critically affect the separation behavior [114]. Relatively thick GO membranes (~3-7 nm) were also prepared by Kim and co-workers on polyethersulfone (PES) via spin-coating and resulted in highly CO_2-philic permeation behavior which was further enhanced by the presence of water. These membranes exhibited CO_2 permeability of ~8500 Barrer and CO_2/N_2 selectivity of 20 under dry conditions and ~ 90 under humidified conditions. Li et al. prepared ultrathin GO membranes on anodic aluminum oxide supports for selective hydrogen separation [113]. The fabrication procedure via filtration led to selective layers approaching 1.8 nm in thickness and selectivity values as high as 3400 and 900 for H_2/CO_2 and H_2/N_2, respectively. The authors of this work speculated that the major transport pathway for H_2 and He molecules was structural defects within GO flakes instead of spacing between the flakes.

Other types of membranes that could be successfully used for gas separation are those based on graphene-polymer composites (Figure 6). To the best of our knowledge there are few works which subtly address gas separation and are mainly focused on gas barrier properties of such materials [115, 116]. It has been recently published the preparation of a nanometre thick GO-polyethylenimine (PEI) film via layer-by-layer assembly for its application as impermeable coating with a H_2/CO_2 selectivity higher than 383 [115]. Polycarbonate (PC) films reinforced with graphite and functionalized graphene sheets (FGS) were also fabricated via melt compounding and showed that both fillers were able of suppressing N_2 and He permeation although FGS was slightly better [116]. It was also observed that N_2 was blocked more efficiently than He in FGS-PC films due to the presence of atomistic perforations formed during pyrolysis treatments which suggests their potential for gas separation. As already mentioned the incorporation of impermeable materials such as graphene into polymers can reduce the permeation rate of gas molecules diffusing through them, graphene fillers in polymers have been investigated for enhancing gas barrier properties of polymer films [117-123]. However, there is also enormous potential for gas separation with graphene-based

MMMs as graphene and graphene-like materials can also be selective to certain gases [31, 113, 115, 116]. Regarding this matter it is worth mentioning that graphene has already been successfully used to produce nanofiltration and pervaporation polymer composite membranes; PES nanofiltration MMMS containing GO have been prepared for antifouling proposes [124]. Solvent resistant nanofiltration membranes with much higher permeances have also been fabricated by dispersing GO into the polymer matrix [125]. Highly oxygenated surface FGSs were incorporated into sodium alginate membranes for dehydration of isopropyl alcohol via pervaporation and high permeance and selectivity values were achieved [126]. Crystalline flake graphite MMMs were fabricated and tested for pervaporation of benzene and cyclohexane mixtures. These hybrid membranes showed about 4-fold permeation flux and 6-fold separation factor increase in comparison to pure PVA membrane [127].

Conclusions and outlook

The interest in membrane technology for separation processes is undeniable because of some outstanding advantages compared to traditional methods such as ease operation, reduced energy consumption and environmentally friendly. It is therefore not surprising that the U.S. market for products related to membranes used in gas separation, pervaporation and novel processes is predicted to grow at an annual rate of 6.6%, from an estimated 180 million USD in 2010 to 247 million USD in 2015 [128].

Scaling up processes and reproducibility from laboratory conditions to industrial production are perhaps the major limitations that many types of membranes, especially inorganic membranes, suffer from. MMMs combine the processability of polymers with the exceptional separation properties of fillers. Thus several of the already developed techniques for manufacturing polymeric membranes can be applied to MMMs. For example, a well-developed technology for the processing of polymers such as melt compounding was applied to obtain MMMs with layered materials [86]. This is a process which, in the case of the layered materials studied here, may also produce their direct exfoliation without the use of organic solvents. Therefore, this represents being an environmentally friendly and scalable method for incorporating nanoplatelets to polymer matrices.

In addition, the high aspect ratio and nanoscale of these materials open the door to introducing them into an asymmetric hollow fiber [34] to create ultrathin selective layers. In any event, it should be noted that the particle orientation is a critical factor in

the separation performance, these materials could make that possible, thus it should be controlled during the chosen membrane fabrication strategy. Other interesting advantages of MMMs with layered fillers are that in most cases the filler loading does not have to be very high to produce a significant permeation effect and the filler increases the thermal stability of the produced nanocomposite membrane.

As discussed along the text, MMMs based on layered and delaminated materials are good candidates to separate CO_2 and H_2 from different gas mixtures, in most of the cases these materials retain their structure and therefore their pore system to act as molecular sieves, sometimes creating a tortuous path for larger molecules due to their high aspect ratio. The usual behavior is that as the amount of filler loading increases (at least until a certain optimum value) the separation performance of pure polymer improves (Figures 7 and 8). However, to overcome the limitations of the Robeson's upper bound [10] the combination of layered and delaminated materials with new classes of polymers (as close to the upper bound as possible) is needed. Among possible candidates, copolyimides [85] (see Figure 7 using 6FDA based polymers) and probably in the near future thermally rearranged (TR) polymers and polymers of intrinsic microporosity (PIMs) [129]. Another idea to keep in mind is the combination of fillers of different nature to approach the attractive zone in the Robeson diagram [27]; highly selective inorganic sheets (JDF-L1) have already been combined with highly permeable silica [26]. The use of graphene in these possible combinations, given the potential high selectivity of this material, could give rise to very interesting MMMs.

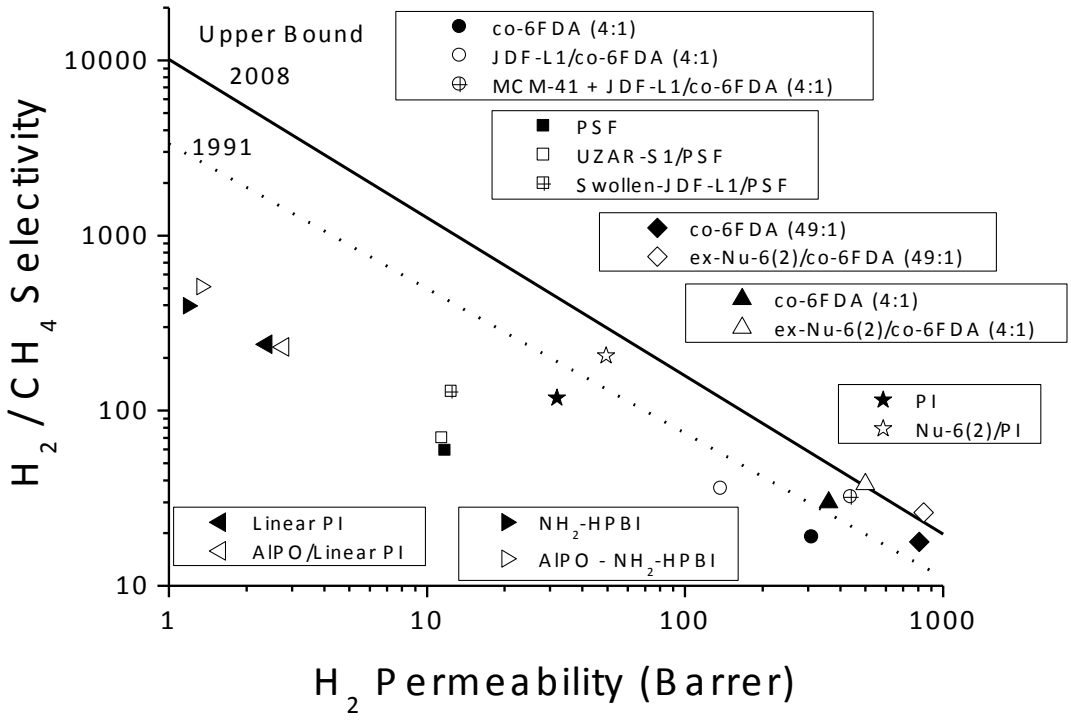

Figure 7. Robeson plot [10] corresponding to the H_2/CH_4 separation with membranes reported in the literature: 4 wt% UZAR-S1/PSF [57], 8.3 wt% swollen JDF-L1/PSF [86], 10 wt% JDF-L1/co-6FDA (4:1) [26], 8 wt% MCM-41 + 4 wt% JDF-L1/co-6FDA (4:1) [26], 5.2-6.2 wt% exfoliated Nu-6(2)/co-6FDA (4:1 and 49:1) [65], 15 wt% Nu-6(2)/PI [64] and 5 wt% AlPO with two different polymer (linear PI and NH_2-HPBI) [36]. Pure polymers are closed symbols and MMMs are open or with cross symbols.

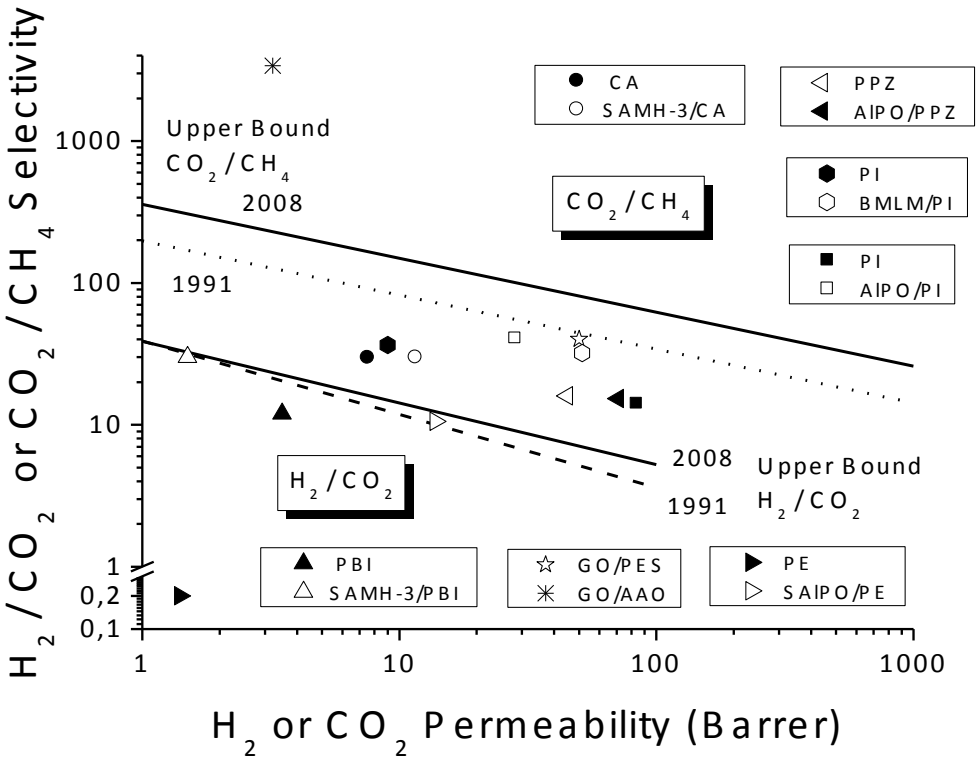

Figure 8. Robeson plot [10] corresponding to the H_2/CO_2 and CO_2/CH_4 separations membranes reported in the literature: 10 wt% AlPO/PI [24], 6 wt% SAMH-3/CA [62], 25 wt% AlPO/substituted polyphosphazene (PPZ) [130], 24 wt% bulk MFI-layered MFI- (BMLM)/PI [54], 2 wt% SAMH-3/PBI [35], GO (3-10 nm)/PES [31], GO (9 nm)/anodic aluminum oxide (AAO) [113] and 5 wt% swollen AlPO/PE [66]. Pure polymers are closed symbols and MMMs are open symbols.

Of course possible new layered and delayered materials could be good candidates as fillers for MMMs. In fact, classical zeolites (e.g. ferrierite, sodalite and MFI) have been recognized as having a layered precursor and this has been suggested as a common possibility to all zeolites [131]. Layered MFI has already been successfully applied to MMMs [54]. On the other hand, the use of crystalline and porous materials built from metal ions as connectors and organic bridging ligands as linkers (metal-organic frameworks, MOFs [132, 133]) are a promising next-generation of membranes for gas separation [22]. Compared to traditional fillers, the interaction between materials should be easier to control in this case due to the better affinity of the MOF linkers with the polymer chains. Layered MOFs [134] are already existing materials and their application in MMMs is something happening soon. Furthermore, graphene and related materials are brought into new applications, such as the preparation of ultrathin GO

membranes by deposition on PES [31] or on anodic aluminum oxide [113] supports that give very interesting separation properties with high selectivities for hydrogen separation (Figures 7 and 8).

Finally, in the development of membrane applications it should be considered not only the development of materials, including experimental, characterization, modeling and simulation aspects [135], but also effective process design [136]. Taking into account all these factors membrane technologies could be economically and environmentally competitive compared to traditional processes. In addition, nowadays and in the coming years, the technology developed for this kind of membranes could be applied to many other systems where it might be necessary a device that selectively discriminate, separate or control the transport of certain compounds, other gas separations from those involving H_2 and CO_2 (e.g. oxygen/nitrogen, olefin/paraffin), pervaporation applications, barrier effect, ultrafiltration, nanofiltration, fuel cells, delivery systems, packaging and gas sensing.

List of abbreviations

4MPD	2,3,5,6-tetramethyl-1,4-phenylenediamine
6FDA	4,4'-hexafluoroisopropylidene diphthalic acid anhydride
AAO	Anodic aluminum oxide
AlPO	Layered aluminophosfate
BET	Brunauer–Emmett–Teller
BMLM	Bulk MFI-layered MFI
CA	Cellulose acetate
co-6FDA	4,4'-hexafluoroisopropylidene diphthalic, anhydride, coopolyimide, i.e. 6FDA-4MPD/6FDA-DABA
CTA	Cetyl trimethyl ammonium
CVD-G	Chemical vapor deposition graphene
DABA	3,5-diaminobenzoic acid
DDA	Dodecylamine
EISA	Evaporation induced self-assembly
FFV	Fractional free volume
FGS	Functionalized graphene sheets
FIB	Focused ion beam
FLG	Few-layered graphene

GO	Graphene oxide
HPBI	2-(2'-hydroxyphenyl) benzimidazole
LBL	Layer-by-layer
MCM	Mobil composition of matter
MD	Molecular dynamics
MMM	Mixed matrix membrane
MOF	Metal organic framework
MR	Membered ring
ODA	Octadecylamine
OPT	Octahedral-pentahedral-tetrahedral
OSDA	Organic structure-directing agent
PBI	Polybenzimidazole
PC	Polycarbonate
PDMS	Polydimethylsiloxane
PE	Polyethylene
PEI	Polyetherimide
PES	Polyethersulfone
PI	Polyimide
PIM	Polymer of intrinsic microporosity
PMMA	Poly(methyl methacrylate)
POM	Partial oxidation of methane
PPZ	Polyphosphazene
PS	Polystyrene
PSF	Polysulfone
PTMSP	Poly(1-methylsilyl-1-propyne)
rGO	Reduced graphene oxide
SAMH-3	Swollen AMH-3
SAXS	Small-angle X-ray scattering
SEM	Scanning electron microscope
SPT	Silica-pillared H+-titanosilicate
TEM	Transmission electron microscopy
TEOS	Tetraethyl orthosilicate
TR	Thermally rearranged
USD	United States dollar

XRD X-ray diffraction

Acknowledgments

We would like to thank the Spanish Ministry of Economy and Competitiveness (MAT2010-15870, IPT-2011-0878-420000) and the Aragón Government and the ESF. We acknowledge the use of facilities within the Laboratorio de Microscopías Avanzadas at Instituto de Nanociencia de Aragon, where the electron microscopy works have been conducted, and the use of Servicio General de Apoyo a la Investigación-SAI (Universidad de Zaragoza).

References

[1] Armor, J.N. The multiple roles for catalysis in the production of H_2. *Appl. Catal. A-Gen.*, **1999**, *176*, 159-176.
[2] Sircar, S.; Golden, T.C. Purification of hydrogen by pressure swing adsorption. *Sep. Sci. Technol.* , **2000**, *35*, 667-687.
[3] Hinchliffe, A.B.; Porter, K.E. A comparison of membrane separation and distillation. *Chem. Eng. Res. Des.*, **2000**, *78*, 255-268.
[4] Samanta, A.; Zhao, A.; Shimizu, G.K.H.; Sarkar, P.; Gupta, R. Post-Combustion CO_2 Capture Using Solid Sorbents: A Review. *Ind. Eng. Chem. Res.*, **2012**, *51*, 1438-1463.
[5] Cobden, P.D.; van Beurden, P.; Reijers, H.T.J.; Elzinga, G.D.; Kluiters, S.C.A.; Dijkstra, J.W.; Jansen, D.; van den Brink, R.W. Sorption-enhanced hydrogen production for pre-combustion CO_2 capture: Thermodynamic analysis and experimental results. *Int. J. Greenh. Gas. Con.*, **2007**, *1*, 170-179.
[6] Lape, N.K.; Nuxoll, E.E.; Cussler, E.L. Polydisperse flakes in barrier films. *J. Membr. Sci.*, **2004**, *236*, 29-37.
[7] Engels, S.; Beggel, F.; Modigell, M.; Stadler, H. Simulation of a membrane unit for oxyfuel power plants under consideration of realistic BSCF membrane properties. *J. Membr. Sci.*, **2010**, *359*, 93-101.
[8] Chung, T.S. A review of microporous composite polymeric membrane technology for air-separation. *Polym. Polym. Compos.*, **1996**, *4*, 269-283.
[9] Baker, R.W. Future directions of membrane gas separation technology. *Ind. Eng. Chem. Res.*, **2002**, *41*, 1393-1411.
[10] Robeson, L.M. The upper bound revisited. *J. Membr. Sci.*, **2008**, *320*, 390-400.
[11] Bernardo, P.; Drioli, E.; Golemme, G. Membrane Gas Separation: A Review/State of the Art. *Ind. Eng. Chem. Res.*, **2009**, *48*, 4638-4663.
[12] Lin, H.Q.; Van Wagner, E.; Freeman, B.D.; Toy, L.G.; Gupta, R.P. Plasticization-enhanced hydrogen purification using polymeric membranes. *Science*, **2006**, *311*, 639-642.
[13] Shao, L.; Low, B.T.; Chung, T.S.; Greenberg, A.R. Polymeric membranes for the hydrogen economy: Contemporary approaches and prospects for the future. *J. Membr. Sci.*, **2009**, *327*, 18-31.
[14] Charpentier, J.C. Modern chemical engineering in the framework of globalization, sustainability, and technical innovation. *Ind. Eng. Chem. Res.*, **2007**, *46*, 3465-3485.

[15] Chung, T.S.; Jiang, L.Y.; Li, Y.; Kulprathipanja, S. Mixed matrix membranes (MMMs) comprising organic polymers with dispersed inorganic fillers for gas separation. *Prog. Polym. Sci.*, **2007**, *32*, 483-507.
[16] Vu, D.Q.; Koros, W.J.; Miller, S.J. Mixed matrix membranes using carbon molecular sieves - I. Preparation and experimental results. *J. Membr. Sci.*, **2003**, *211*, 311-334.
[17] Mahajan, R.; Vu, D.Q.; Koros, W.J. Mixed matrix membrane materials: An answer to the challenges faced by membrane based gas separations today? *J. Chin. Inst. Chem. Eng.*, **2002**, *33*, 77-86.
[18] Reid, B.D.; Ruiz-Trevino, A.; Musselman, I.H.; Balkus, K.J.; Ferraris, J.P. Gas permeability properties of polysulfone membranes containing the mesoporous molecular sieve MCM-41. *Chem. Mater.*, **2001**, *13*, 2366-2373.
[19] Choi, S.; Coronas, J.; Sheffel, J.A.; Jordan, E.; Oh, W.; Nair, S.; Shantz, D.F.; Tsapatsis, M. Layered silicate by proton exchange and swelling of AMH-3. *Microporous Mesoporous Mater.*, **2008**, *115*, 75-84.
[20] Zhang, Y.F.; Musseman, I.H.; Ferraris, J.P.; Balkus, K.J. Gas permeability properties of Matrimid (R) membranes containing the metal-organic framework Cu-BPY-HFS. *J. Membr. Sci.*, **2008**, *313*, 170-181.
[21] Zornoza, B.; Irusta, S.; Tellez, C.; Coronas, J. Mesoporous Silica Sphere-Polysulfone Mixed Matrix Membranes for Gas Separation. *Langmuir*, **2009**, *25*, 5903-5909.
[22] Zornoza, B.; Tellez, C.; Coronas, J.; Gascon, J.; Kapteijn, F. Metal organic framework based mixed matrix membranes: An increasingly important field of research with a large application potential. *Microporous Mesoporous Mater.*, **2013**, *166*, 67-78.
[23] Zornoza, B.; Esekhile, O.; Koros, W.J.; Tellez, C.; Coronas, J. Hollow silicalite-1 sphere-polymer mixed matrix membranes for gas separation. *Sep. Purif. Technol.*, **2011**, *77*, 137-145.
[24] Jeong, H.K.; Krych, W.; Ramanan, H.; Nair, S.; Marand, E.; Tsapatsis, M. Fabrication of polymer/selective-flake nanocomposite membranes and their use in gas separation. *Chem. Mater.*, **2004**, *16*, 3838-3845.
[25] Sorribas, S.; Gorgojo, P.; Tellez, C.; Coronas, J.; Livingston, A.G. High Flux Thin Film Nanocomposite Membranes Based on Metal-Organic Frameworks for Organic Solvent Nanofiltration. *J. Am. Chem. Soc.*, **2013**, *135*, 15201-15208.
[26] Galve, A.; Sieffert, D.; Staudt, C.; Ferrando, M.; Guell, C.; Tellez, C.; Coronas, J. Combination of ordered mesoporous silica MCM-41 and layered titanosilicate JDF-L1 fillers for 6FDA-based copolyimide mixed matrix membranes. *J. Membr. Sci.*, **2013**, *431*, 163-170.
[27] Zornoza, B.; Seoane, B.; Zamaro, J.M.; Téllez, C.; Coronas, J. Combination of MOFs and Zeolites for Mixed-Matrix Membranes. *ChemPhysChem*, **2011**, *12*, 2781-2785.
[28] Alexandre, M.; Dubois, P. Polymer-layered silicate nanocomposites: preparation, properties and uses of a new class of materials. *Mat. Sci. Eng. R* **2000**, *28*, 1-63.
[29] Goh, P.S.; Ismail, A.F.; Sanip, S.M.; Ng, B.C.; Aziz, M. Recent advances of inorganic fillers in mixed matrix membrane for gas separation. *Sep. Purif. Technol.*, **2011**, *81*, 243-264.
[30] Gascon, J.; Kapteijn, F.; Zornoza, B.; Sebastian, V.; Casado, C.; Coronas, J. Practical Approach to Zeolitic Membranes and Coatings: State of the Art, Opportunities, Barriers, and Future Perspectives. *Chem. Mater.*, **2012**, *24*, 2829-2844.
[31] Kim, H.W.; Yoon, H.W.; Yoon, S.-M.; Yoo, B.M.; Ahn, B.K.; Cho, Y.H.; Shin, H.J.; Yang, H.; Paik, U.; Kwon, S.; Choi, J.-Y.; Park, H.B. Selective Gas Transport

Through Few-Layered Graphene and Graphene Oxide Membranes. *Science*, **2013**, *342*, 91-95.
[32] Rubio, C.; Casado, C.; Uriel, S.; Tellez, C.; Coronas, J. Seeded synthesis of layered titanosilicate JDF-L1. *Mater. Lett.*, **2009**, *63*, 113-115.
[33] Leon, V.; Quintana, M.; Herrero, M.A.; Fierro, J.L.G.; de la Hoz, A.; Prato, M.; Vazquez, E. Few-layer graphenes from ball-milling of graphite with melamine. *Chem. Commun.*, **2011**, *47*, 10936-10938.
[34] Johnson, J.R.; Koros, W.J. Utilization of nanoplatelets in organic-inorganic hybrid separation materials: Separation advantages and formation challenges. *J. Taiwan Inst. Chem. E.*, **2009**, *40*, 268-275.
[35] Choi, S.; Coronas, J.; Jordan, E.; Oh, W.; Nair, S.; Onorato, F.; Shantz, D.F.; Tsapatsis, M. Layered silicates by swelling of AMH-3 and nanocomposite membranes. *Angew. Chem. Int. Edit.*, **2008**, *47*, 552-555.
[36] Vaughan, B.R.; Marand, E. Transport properties of polymer–aluminophosphate nano-composites prepared by simple mixing. *J. Membr. Sci.*, **2008**, *310*, 197-207.
[37] Zornoza, B.; Gorgojo, P.; Casado, C.; Téllez, C.; Coronas, J. Mixed matrix membranes for gas separation with special nanoporous fillers. *Desalin. Water Treat.*, **2011**, *27*, 42-47.
[38] Aguzzi, C.; Cerezo, P.; Viseras, C.; Caramella, C. Use of clays as drug delivery systems: Possibilities and limitations. *Appl. Clay Sci.*, **2007**, *36*, 22-36.
[39] Choy, J.H.; Choi, S.J.; Oh, J.M.; Park, T. Clay minerals and layered double hydroxides for novel biological applications. *Appl. Clay Sci.*, **2007**, *36*, 122-132.
[40] Dong, Y.; Feng, S.S. Poly(d,l-lactide-co-glycolide)/montmorillonite nanoparticles for oral delivery of anticancer drugs. *Biomaterials*, **2005**, *26*, 6068-6076.
[41] Corma, A.; Fornes, V.; Guil, J.M.; Pergher, S.; Maesen, T.L.M.; Buglass, J.G. Preparation, characterisation and catalytic activity of ITQ-2, a delaminated zeolite. *Microporous Mesoporous Mater.*, **2000**, *38*, 301-309.
[42] Gorgojo, P.; Galve, A.; Uriel, S.; Tellez, C.; Coronas, J. Direct exfoliation of layered zeolite Nu-6(1). *Microporous Mesoporous Mater.*, **2011**, *142*, 122-129.
[43] Corma, A.; Fornes, V.; Pergher, S.B.; Maesen, T.L.M.; Buglass, J.G. Delaminated zeolite precursors as selective acidic catalysts. *Nature*, **1998**, *396*, 353-356.
[44] Medina, M.E.; Iglesias, M.; Gutierrez-Puebla, E.; Monge, M.A. Solvothermal synthesis and structural relations among three anionic aluminophosphates; catalytic behaviour. *J. Mater. Chem.*, **2004**, *14*, 845-850.
[45] Corma, A.; Fornes, V.; Rey, F. Delaminated zeolites: An efficient support for enzymes. *Adv. Mater.*, **2002**, *14*, 71-74.
[46] Zukal, A.; Dominguez, I.; Mayerova, J.; Cejka, J. Functionalization of Delaminated Zeolite ITQ-6 for the Adsorption of Carbon Dioxide. *Langmuir*, **2009**, *25*, 10314-10321.
[47] Cussler, E.L. Membranes containing selective flakes. *J. Membr. Sci.*, **1990**, *52*, 275-288.
[48] Sheffel, J.A.; Tsapatsis, M. A model for the performance of microporous mixed matrix membranes with oriented selective flakes. *J. Membr. Sci.*, **2007**, *295*, 50-70.
[49] Lawton, S.; Leonowicz, M.E.; Partridge, R.; Chu, P.; Rubin, M.K. Twelve-ring pockets on the external surface of MCM-22 crystals. *Microporous Mesoporous Mater.*, **1998**, *23*, 109-117.
[50] Schreyeck, L.; Caullet, P.; Mougenel, J.C.; Guth, J.L.; Marler, B. A new layered (alumino) silicate precursor of FER-type zeolite. *Microporous Mater.*, **1996**, *6*, 259-271.

[51] Zanardi, S.; Alberti, A.; Cruciani, G.; Corma, A.; Fornes, V.; Brunelli, M. Crystal structure determination of zeolite Nu-6(2) and its layered precursor Nu-6(1). *Angew. Chem.Int. Edit.*, **2004**, *43*, 4933-4937.
[52] Corma, A.; Diaz, U.; Domine, M.E.; Fornes, V. New aluminosilicate and titanosilicate delaminated materials active for acid catalysis, and oxidation reactions using H_2O_2. *J. Am. Chem. Soc.*, **2000**, *122*, 2804-2809.
[53] Corma, A.; Fornes, V.; Diaz, U. ITQ-18 a new delaminated stable zeolite. *Chem. Commun.*, **2001**, 2642-2643.
[54] Kim, W.G.; Zhang, X.Y.; Lee, J.S.; Tsapatsis, M.; Nair, S. Epitaxially Grown Layered MFI - Bulk MFI Hybrid Zeolitic Materials. *ACS Nano*, **2012**, *6*, 9978-9988.
[55] Jeong, H.K.; Nair, S.; Vogt, T.; Dickinson, L.C.; Tsapatsis, M. A highly crystalline layered silicate with three-dimensionally microporous layers. *Nat. Mater.*, **2003**, *2*, 53-58.
[56] Pinnavaia, T.J. Intercalated Clay Catalysts. *Science*, **1983**, *220*, 365-371.
[57] Rubio, C.; Casado, C.; Gorgojo, P.; Etayo, F.; Uriel, S.; Tellez, C.; Coronas, J. Exfoliated Titanosilicate Material UZAR-S1 Obtained from JDF-L1. *Eur. J. Inorg. Chem.*, **2010**, *2010*, 159-163.
[58] Rezakazemi, M.; Ebadi Amooghin, A.; Montazer-Rahmati, M.M.; Ismail, A.F.; Matsuura, T. State-of-the-art membrane based CO2 separation using mixed matrix membranes (MMMs): An overview on current status and future directions. *Prog. Polym. Sci.*, **2014**, *39*, 817-861.
[59] Defontaine, G.; Barichard, A.; Letaief, S.; Feng, C.; Matsuura, T.; Detellier, C. Nanoporous polymer – Clay hybrid membranes for gas separation. *J. Colloid Interface Sci.*, **2010**, *343*, 622-627.
[60] Hashemifard, S.A.; Ismail, A.F.; Matsuura, T. Effects of montmorillonite nano-clay fillers on PEI mixed matrix membrane for CO_2 removal. *Chem. Eng. J.*, **2011**, *170*, 316-325.
[61] Choi, S.; Coronas, J.; Lai, Z.; Yust, D.; Onorato, F.; Tsapatsis, M. Fabrication and gas separation properties of polybenzimidazole (PBI)/nanoporous silicates hybrid membranes. *J. Membr. Sci.*, **2008**, *316*, 145-152.
[62] Kim, W.G.; Lee, J.S.; Bucknall, D.G.; Koros, W.J.; Nair, S. Nanoporous layered silicate AMH-3/cellulose acetate nanocomposite membranes for gas separations. *J. Membr. Sci.*, **2013**, *441*, 129-136.
[63] Gorgojo, P.; Uriel, S.; Téllez, C.; Coronas, J. Development of mixed matrix membranes based on zeolite Nu-6(2) for gas separation. *Microporous Mesoporous Mater.*, **2008**, *115*, 85-92.
[64] Gorgojo, P.; Zornoza, B.; Uriel, S.; Tellez, C.; Coronas, J. Mixed Matrix Membranes from Nanostructured Materials for Gas Separation. In: *Zeolites and Related Materials: Trends, Targets and Challenges, Proceedings of the 4th International Feza Conference*, A. Gedeon, P. Massiani and F. Babonneau, Eds.; Elsevier Science Bv: Amsterdam, **2008;** Vol. *174*, pp 653-656.
[65] Gorgojo, P.; Sieffert, D.; Staudt, C.; Tellez, C.; Coronas, J. Exfoliated zeolite Nu-6(2) as filler for 6FDA-based copolyimide mixed matrix membranes. *J. Membr. Sci.*, **2012**, *411*, 146-152.
[66] Covarrubias, C.; Quijada, R. Preparation of aluminophosphate/polyethylene nanocomposite membranes and their gas permeation properties. *J. Membr. Sci.*, **2010**, *358*, 33-42.
[67] Pavlidou, S.; Papaspyrides, C.D. A review on polymer–layered silicate nanocomposites. *Prog. Polym. Sci.*, **2008**, *33*, 1119-1198.

[68] Sinha Ray, S.; Okamoto, M. Polymer/layered silicate nanocomposites: a review from preparation to processing. *Prog. Polym. Sci.*, **2003**, *28*, 1539-1641.
[69] He, Y.J.; Nivarthy, G.S.; Eder, F.; Seshan, K.; Lercher, J.A. Synthesis, characterization and catalytic activity of the pillared molecular sieve MCM-36. *Microporous Mesoporous Mater.*, **1998**, *25*, 207-224.
[70] Choi, J.; Tsapatsis, M. MCM-22/Silica Selective Flake Nanocomposite Membranes for Hydrogen Separations. *J. Am. Chem. Soc.*, **2010**, *132*, 448-449.
[71] Whittam, T.V. U.S. Patent 4 397 825, **1983**.
[72] Lawton, S.L.; Fung, A.S.; Kennedy, G.J.; Alemany, L.B.; Chang, C.D.; Hatzikos, G.H.; Lissy, D.N.; Rubin, M.K.; Timken, H.K.C.; Steuernagel, S.; Woessner, D.E. Zeolite MCM-49: A three-dimensional MCM-22 analogue synthesized by in situ crystallization. *J. Phys. Chem.*, **1996**, *100*, 3788-3798.
[73] Varoon, K.; Zhang, X.Y.; Elyassi, B.; Brewer, D.D.; Gettel, M.; Kumar, S.; Lee, J.A.; Maheshwari, S.; Mittal, A.; Sung, C.Y.; Cococcioni, M.; Francis, L.F.; McCormick, A.V.; Mkhoyan, K.A.; Tsapatsis, M. Dispersible Exfoliated Zeolite Nanosheets and Their Application as a Selective Membrane. *Science*, **2011**, *334*, 72-75.
[74] Thomas, J.M.; Jones, R.H.; Xu, R.R.; Chen, J.S.; Chippindale, A.M.; Natarajan, S.; Cheetham, A.K. A Novel Porous Sheet Aluminophosphate - $Al_3P_4O_{16}^{3-}$ $1.5[NH_3(CH_2)_4NH_3]^{2+}$. *J. Chem. Soc., Chem. Commun.*, **1992**, 929-931.
[75] Gao, Q.M.; Li, B.Z.; Chen, J.S.; Li, S.G.; Xu, R.R.; Williams, I.; Zheng, J.Q.; Barber, D. Nonaqueous synthesis and characterization of a new 2-dimensional layered aluminophosphate $[Al_3P_4O_{16}]^{3-}\cdot 3[CH_3CH_2NH_3]^{+}$. *J. Solid State Chem.*, **1997**, *129*, 37-44.
[76] Rocha, J.; Anderson, M.W. Microporous titanosilicates and other novel mixed octahedral-tetrahedral framework oxides. *Eur. J. Inorg. Chem.*, **2000**, *2000*, 801-818.
[77] Anderson, M.W.; Terasaki, O.; Ohsuna, T.; Philippou, A.; Mackay, S.P.; Ferreira, A.; Rocha, J.; Lidin, S. Structure of the microporous titanosilicate ETS-10. *Nature*, **1994**, *367*, 347-351.
[78] Philippou, A.; Anderson, M.W. Structural investigation of ETS-4. *Zeolites*, **1996**, *16*, 98-107.
[79] Lin, Z.; Rocha, J.; Brandao, P.; Ferreira, A.; Esculcas, A.P.; deJesus, J.D.P.; Philippou, A.; Anderson, M.W. Synthesis and structural characterization of microporous umbite, penkvilksite, and other titanosilicates. *J. Phys. Chem. B*, **1997**, *101*, 7114-7120.
[80] Roberts, M.A.; Sankar, G.; Thomas, J.M.; Jones, R.H.; Du, H.; Chen, J.; Pang, W.; Xu, R. Synthesis and structure of a layered titanosilicate catalyst with five-coordinate titanium. *Nature*, **1996**, *381*, 401-404.
[81] Krivovichev, S.V.; Armbruster, T. The crystal structure of jonesite, $Ba_2(K,Na)[Ti_2(Si_5Al)O_{18}(H2O)](H_2O)_n$: A first example of titanosilicate with porous double layers. *Am. Miner.*, **2004**, *89*, 314-318.
[82] Anderson, M.W.; Terasaki, O.; Ohsuna, T.; Malley, P.J.O.; Philippou, A.; Mackay, S.P.; Ferreira, A.; Rocha, J.; Lidin, S. Microporous titanosilicate ETS-10: A structural survey. *Philos. Mag. B* **1995**, *71*, 813-841.
[83] Veltri, M.; Vuono, D.; De Luca, P.; Nagy, J.B.; Nastro, A. Typical data of a new microporous material obtained from gels with titanium and silicon. *J. Therm. Anal. Calorim.*, **2006**, *84*, 247-252.
[84] Ferdov, S.; Kostov-Kytin, V.; Petrov, O. A rapid method of synthesizing the layered titanosilicate JDF-L1. *Chem. Commun.*, **2002**, 1786-1787.

[85] Galve, A.; Sieffert, D.; Vispe, E.; Tellez, C.; Coronas, J.; Staudt, C. Copolyimide mixed matrix membranes with oriented microporous titanosilicate JDF-L1 sheet particles. *J. Membr. Sci.*, **2011**, *370*, 131-140.
[86] Castarlenas, S.; Gorgojo, P.; Casado-Coterillo, C.; Masheshwari, S.; Tsapatsis, M.; Tellez, C.; Coronas, J. Melt Compounding of Swollen Titanosilicate JDF-L1 with Polysulfone To Obtain Mixed Matrix Membranes for H_2/CH_4 Separation. *Ind. Eng. Chem. Res.*, **2013**, *52*, 1901-1907.
[87] Zornoza, B.; Téllez, C.; Coronas, J. Mixed matrix membranes comprising glassy polymers and dispersed mesoporous silica spheres for gas separation. *J. Membr. Sci.*, **2011**, *368*, 100-109.
[88] Pérez-Carvajal, J.; Aranda, P.; Berenguer-Murcia, A.; Cazorla-Amorós, D.; Coronas, J.n.; Ruiz-Hitzky, E. Nanoarchitectures Based on Layered Titanosilicates Supported on Glass Fibers: Application to Hydrogen Storage. *Langmuir*, **2012**, *29*, 7449-7455.
[89] Park, K.-W.; Jung, J.H.; Kim, J.D.; Kim, S.-K.; Kwon, O.-Y. Preparation of mesoporous silica-pillared H^+-titanosilicates. *Microporous Mesoporous Mater.*, **2009**, *118*, 100-105.
[90] Park, K.-W.; Seo, H.J.; Kwon, O.-Y. Mesoporous silica-pillared titanosilicate as catalytic support for partial oxidation of methane. *Microporous Mesoporous Mater.*, **2014**, 191-196.
[91] Dadachov, M.S.; Rocha, J.; Ferreira, A.; Lin, Z.; Anderson, M.W. Ab initio structure determination of layered sodium titanium silicate containing edge-sharing titanate chains (AM-4) $Na_3(Na,H)Ti_2O_2[Si_2O_6]\cdot 2.2H_2O$. *Chem. Commun.*, **1997**, 2371-2372.
[92] Casado, C.; Ambroj, D.; Mayoral, A.; Vispe, E.; Tellez, C.; Coronas, J. Synthesis, swelling, and exfoliation of microporous lamellar titanosilicate AM-4. *Eur. J. Inorg. Chem.*, **2011**, *2011*, 2247-2253.
[93] Anson, A.; Lin, C.C.H.; Kuznicki, S.M.; Sawada, J.A. Adsorption of carbon dioxide, ethane, and methane on titanosilicate type molecular sieves. *Chem. Eng. Sci.*, **2009**, *64*, 3683-3687.
[94] Lima, S.; Dias, A.S.; Lin, Z.; Brandao, P.; Ferreira, P.; Pillinger, M.; Rocha, J.; Calvino-Casilda, V.; Valente, A.A. Isomerization of D-glucose to D-fructose over metallosilicate solid bases. *Appl. Catal. A-Gen.*, **2008**, *339*, 21-27.
[95] Pérez-Carvajal, J.; Lalueza, P.; Casado, C.; Téllez, C.; Coronas, J. Layered titanosilicates JDF-L1 and AM-4 for biocide applications. *Appl. Clay. Sci.*, **2012**, *56*, 30-35.
[96] Novoselov, K.S.; Geim, A.K.; Morozov, S.V.; Jiang, D.; Zhang, Y.; Dubonos, S.V.; Grigorieva, I.V.; Firsov, A.A. Electric field effect in atomically thin carbon films. *Science*, **2004**, *306*, 666-669.
[97] Spitalsky, Z.; Danko, M.; Mosnacek, J. Preparation of Functionalized Graphene Sheets. *Curr. Org. Chem.*, **2011**, *15*, 1133-1150.
[98] Berry, V. Impermeability of graphene and its applications. *Carbon*, **2013**, *62*, 1-10.
[99] Nair, R.R.; Wu, H.A.; Jayaram, P.N.; Grigorieva, I.V.; Geim, A.K. Unimpeded Permeation of Water Through Helium-Leak-Tight Graphene-Based Membranes. *Science*, **2012**, *335*, 442-444.
[100] Joshi, R.K.; Carbone, P.; Wang, F.C.; Kravets, V.G.; Su, Y.; Grigorieva, I.V.; Wu, H.A.; Geim, A.K.; Nair, R.R. Precise and Ultrafast Molecular Sieving Through Graphene Oxide Membranes. *Science*, **2014**, *343*, 752-754.
[101] Han, Y.; Xu, Z.; Gao, C. Ultrathin Graphene Nanofiltration Membrane for Water Purification. *Adv. Funct. Mater.*, **2013**, *23*, 3693-3700.

[102] Jiang, D.E.; Cooper, V.R.; Dai, S. Porous Graphene as the Ultimate Membrane for Gas Separation. *Nano Lett.*, **2009**, *9*, 4019-4024.
[103] Du, H.; Li, J.; Zhang, J.; Su, G.; Li, X.; Zhao, Y. Separation of Hydrogen and Nitrogen Gases with Porous Graphene Membrane. *J. Phys. Chem. C*, **2011**, *115*, 23261-23266.
[104] Drahushuk, L.W.; Strano, M.S. Mechanisms of Gas Permeation through Single Layer Graphene Membranes. *Langmuir*, **2012**, *28*, 16671-16678.
[105] Shan, M.; Xue, Q.; Jing, N.; Ling, C.; Zhang, T.; Yan, Z.; Zheng, J. Influence of chemical functionalization on the CO_2/N_2 separation performance of porous graphene membranes. *Nanoscale*, **2012**, *4*, 5477-5482.
[106] Lee, J.; Aluru, N.R. Water-solubility-driven separation of gases using graphene membrane. *J. Membr. Sci.*, **2013**, *428*, 546-553.
[107] Liu, H.; Dai, S.; Jiang, D.E. Insights into CO_2/N_2 separation through nanoporous graphene from molecular dynamics. *Nanoscale*, **2013**, *5*, 9984-9987.
[108] Liu, H.; Dai, S.; Jiang, D.E. Permeance of H_2 through porous graphene from molecular dynamics. *Solid State Commun.*, **2013**, *175*, 101-105.
[109] Qin, X.; Meng, Q.; Feng, Y.; Gao, Y. Graphene with line defect as a membrane for gas separation: Design via a first-principles modeling. *Surf. Sci.*, **2013**, *607*, 153-158.
[110] Fischbein, M.D.; Drndic, M. Electron beam nanosculpting of suspended graphene sheets. *Appl. Phys. Lett.*, **2008**, *93*, 1-3.
[111] Koenig, S.P.; Wang, L.; Pellegrino, J.; Bunch, J.S. Selective molecular sieving through porous graphene. *Nat. Nanotechnol.*, **2012**, *7*, 728-732.
[112] Celebi, K.; Buchheim, J.; Wyss, R.M.; Droudian, A.; Gasser, P.; Shorubalko, I.; Kye, J.-I.; Lee, C.; Park, H.G. Ultimate Permeation Across Atomically Thin Porous Graphene. *Science*, **2014**, *344*, 289-292.
[113] Li, H.; Song, Z.; Zhang, X.; Huang, Y.; Li, S.; Mao, Y.; Ploehn, H.J.; Bao, Y.; Yu, M. Ultrathin, Molecular-Sieving Graphene Oxide Membranes for Selective Hydrogen Separation. *Science*, **2013**, *342*, 95-98.
[114] Boutilier, M.S.H.; Sun, C.; O'Hern, S.C.; Au, H.; Hadjiconstantinou, N.G.; Karnik, R. Implications of Permeation through Intrinsic Defects in Graphene on the Design of Defect-Tolerant Membranes for Gas Separation. *ACS Nano*, **2014**, *8*, 841-849.
[115] Yang, Y.H.; Bolling, L.; Priolo, M.A.; Grunlan, J.C. Super Gas Barrier and Selectivity of Graphene Oxide-Polymer Multilayer Thin Films. *Adv. Mater.*, **2013**, *25*, 503-508.
[116] Kim, H.; Macosko, C.W. Processing-property relationships of polycarbonate/graphene composites. *Polymer*, **2009**, *50*, 3797-3809.
[117] Kim, H.; Miura, Y.; Macosko, C.W. Graphene/Polyurethane Nanocomposites for Improved Gas Barrier and Electrical Conductivity. *Chem. Mater.*, **2010**, *22*, 3441-3450.
[118] Compton, O.C.; Kim, S.; Pierre, C.; Torkelson, J.M.; Nguyen, S.T. Crumpled Graphene Nanosheets as Highly Effective Barrier Property Enhancers. *Adv. Mater.*, **2010**, *22*, 4759-4763.
[119] Chang, K.C.; Hsu, C.H.; Lu, H.I.; Ji, W.F.; Chang, C.H.; Li, W.Y.; Chuang, T.L.; Yeh, J.M.; Liu, W.R.; Tsai, M.H. Advanced anticorrosive coatings prepared from electroactive polyimide/graphene nanocomposites with synergistic effects of redox catalytic capability and gas barrier properties. *Express Polym. Lett.*, **2014**, *8*, 243-255.
[120] Jin, J.; Rafiq, R.; Gill, Y.Q.; Song, M. Preparation and characterization of high performance of graphene/nylon nanocomposites. *Eur. Polym. J.*, **2013**, *49*, 2617-2626.

[121] Kuila, T.; Bose, S.; Mishra, A.K.; Khanra, P.; Kim, N.H.; Lee, J.H. Effect of functionalized graphene on the physical properties of linear low density polyethylene nanocomposites. *Polym. Test*, **2012**, *31*, 31-38.
[122] Chang, K.C.; Ji, W.F.; Lai, M.C.; Hsiao, Y.R.; Hsu, C.H.; Chuang, T.L.; Wei, Y.; Yeh, J.M.; Liu, W.R. Synergistic effects of hydrophobicity and gas barrier properties on the anticorrosion property of PMMA nanocomposite coatings embedded with graphene nanosheets. *Polym. Chem.*, **2014**, *5*, 1049-1056.
[123] Kang, H.L.; Zuo, K.H.; Wang, Z.; Zhang, L.Q.; Liu, L.; Guo, B.C. Using a green method to develop graphene oxide/elastomers nanocomposites with combination of high barrier and mechanical performance. *Compos. Sci. Technol.*, **2014**, *92*, 1-8.
[124] Zinadini, S.; Zinatizadeh, A.A.; Rahimi, M.; Vatanpour, V.; Zangeneh, H. Preparation of a novel antifouling mixed matrix PES membrane by embedding graphene oxide nanoplates. *J. Membr. Sci.*, **2014**, *453*, 292-301.
[125] Shao, L.; Cheng, X.Q.; Wang, Z.X.; Ma, J.; Guo, Z.H. Tuning the performance of polypyrrole-based solvent-resistant composite nanofiltration membranes by optimizing polymerization conditions and incorporating graphene oxide. *J. Membr. Sci.*, **2014**, *452*, 82-89.
[126] Suhas, D.P.; Raghu, A.V.; Jeong, H.M.; Aminabhavi, T.M. Graphene-loaded sodium alginate nanocomposite membranes with enhanced isopropanol dehydration performance via a pervaporation technique. *RSC Adv.*, **2013**, *3*, 17120-17130.
[127] Peng, F.B.; Lu, L.Y.; Sun, H.L.; Pan, F.S.; Jiang, Z.Y. Organic-inorganic hybrid membranes with simultaneously enhanced flux and selectivity. *Ind. Eng. Chem. Res.*, **2007**, *46*, 2544-2549.
[128] BCC Market Research Reports: Membrane Technology for Liquid and Gas Separations. http://www.bccresearch.com/market-research/membrane-and-separation-technology/membrane-tech-liquid-gas-separations-mst041e.html (accessed April 29, 2014).
[129] Budd, P.M.; Msayib, K.J.; Tattershall, C.E.; Ghanem, B.S.; Reynolds, K.J.; McKeown, N.B.; Fritsch, D. Gas separation membranes from polymers of intrinsic microporosity. *J. Membr. Sci.*, **2005**, *251*, 263-269.
[130] Jha, P.; Way, J.D. Carbon dioxide selective mixed-matrix membranes formulation and characterization using rubbery substituted polyphosphazene. *J. Membr. Sci.*, **2008**, *324*, 151-161.
[131] Roth, W.J.; Dorset, D.L. Expanded view of zeolite structures and their variability based on layered nature of 3-D frameworks. *Microporous Mesoporous Mater.*, **2011**, *142*, 32-36.
[132] Rowsell, J.L.C.; Yaghi, O.M. Metal-organic frameworks: a new class of porous materials. *Microporous Mesoporous Mater.*, **2004**, *73*, 3-14.
[133] Yaghi, O.M.; O'Keeffe, M.; Ockwig, N.W.; Chae, H.K.; Eddaoudi, M.; Kim, J. Reticular synthesis and the design of new materials. *Nature*, **2003**, *423*, 705-714.
[134] Arslan, H.K.; Shekhah, O.; Wieland, D.C.F.; Paulus, M.; Sternemann, C.; Schroer, M.A.; Tiemeyer, S.; Tolan, M.; Fischer, R.A.; Wöll, C. Intercalation in Layered Metal–Organic Frameworks: Reversible Inclusion of an Extended π-System. *J. Am. Chem. Soc.*, **2011**, *133*, 8158-8161.
[135] Kim, W.G.; Nair, S. Membranes from nanoporous 1D and 2D materials: A review of opportunities, developments, and challenges. *Chem. Eng. Sci.*, **2013**, *104*, 908-924.
[136] Lin, H. Integrated membrane material and process development for gas separation. *Curr. Opin. Chem. Eng.*, **2014**, *4*, 54-61.